Detailed description of the media used in Figure 1. We used four different types of media: **(A) iron-supplemented casein medium (Casein + Fe).** This medium does not require pyoverdine production to reach WT levels of growth yields as *pvdS* grows to similar levels as WT (Figure 1A). Elastase production is necessary for optimal growth in this medium to digest casein. Growth of the *lasR* mutant is severely impaired in this medium (Figure 1A). Similar media have been typically used in sociomicrobiology studies involving WT and *lasR* [1–3]. **(B) iron-depleted CAA medium (CAA + Transferrin).** This medium does not require elastase production to reach WT levels of growth yields as *lasR* grows to similar levels as WT (Figure 1B). However, iron depletion by addition of apo-transferrin causes pyoverdine production to be required for optimal growth levels as *pvdS*, which does not produce pyoverdine (Figure S2B, Figure S2F), has growth deficiency in this medium (Figure 1B). Similar media have been typically used in sociomicrobiology studies involving WT and *pvdS* [4–21]. **(C) iron-depleted casein medium (Casein + Transferrin).** We prepared a medium specifically designed to combine the requirement of both elastase and pyoverdine production. Elastase production is required in this medium as the sole carbon and nitrogen source is casein. Human apo-transferrin is used to deplete the iron and consequently pyoverdine production is observed (Figure S2C, Figure S2G). The requirement of both elastase and pyoverdine for optimal growth in this medium is demonstrated by the fact that both *lasR* and *pvdS* monocultures show growth deficiencies (Figure 1C). **(D) iron-supplemented CAA medium (CAA + Fe).** This medium does not require either elastase or pyoverdine production for optimal growth as both amino acids and iron are provided. This is demonstrated by the fact that the growth levels of all three strains in monoculture are very similar in this medium, indicating that neither the *pvdS* and *lasR* genes (and therefore elastase and pyoverdine) are required to reach the optimal growth yields of the WT (Figure 1D).

In all the experiments in this study, OD_{600}, CFU/ml, total pyoverdine concentration (Abs_{405}), frequency measurements, and the passages to fresh media are taken at 48 hours after inoculation in all four types of media described above. This time point allows cultures to reach stationary phase in each of the four media.

Differences in growth yields for WT across the different media. We observed lower growth yields of the WT in the medium where only pyoverdine is required (Figure 1B), compared to conditions where the two traits are necessary (Figure 1C). A plausible explanation for this difference relies on the potential difference in iron content between the

two media; the casamino acids (CAA) used (BD, Ref: 223050) is low in iron according to both manufacturer and previous studies [22], whereas casein has iron-chelating capacity [23,24] and therefore is expected to have higher iron concentration. Thus, although all iron depleted media were supplemented with the same amount of transferrin (100 μg/ml), the iron availability is expected to be lower in the media containing CAA than in the media containing casein. Indeed, we observed that the pyoverdine production per cell is higher in the medium where only pyoverdine is necessary than in conditions where both traits are required (see below, Figure S2 panels G and H), which is consistent with having different iron availability in the two media.

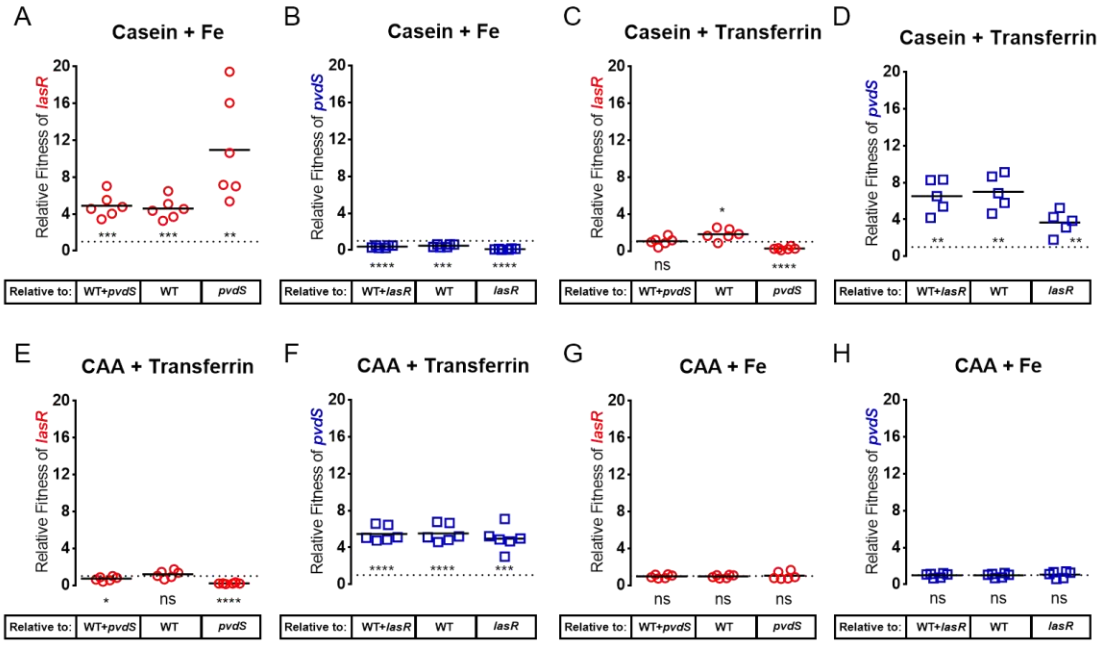

Figure S1 (Related to Figure 2). Relative fitness of *lasR* and *pvdS* in WT+*pvdS*+*lasR* triple co-cultures calculated in respect to the rest of the population (as in Figure 2), or to only WT, or to only the other mutant. Relative fitness (υ) of *lasR* (red circles in **A, C, E,** and **G**), or *pvdS* (blue squares in **B, D, F,** and **H**), calculated in respect to WT+*pvdS*, WT, and *pvdS* after 48 hours of incubation of WT+*pvdS*+*lasR* triple co-cultures in: **(A** and **B)** iron-supplemented casein medium (Casein + Fe), **(C** and **D)** iron-depleted casamino acids medium (CAA + Transferrin), **(E** and **F)** iron-depleted casein medium (Casein + Transferrin), and **(G** and **H)** iron-supplemented casamino acids medium (CAA + Fe). Initial ratios of the strains in WT+*pvdS*+*lasR* triple co-culture are 8:1:1. Dotted lines indicate υ=1. Relative fitness values above the dotted lines (υ>1) indicate that the strain is cheating and below the dotted lines (υ<1) indicate that the strain is being cheated. One-sample t-test was used to determine whether each dataset is significantly different than 1 (significance symbols are located above the dotted line when υ>1 and below the dotted line when υ≤1). Each data point indicates an individual biological replicate (N≥5) and horizontal lines indicate the means of each group. ns=not significant P>0.05, * P≤0.05, ** P≤0.01, *** P≤0.001, **** P≤0.0001.

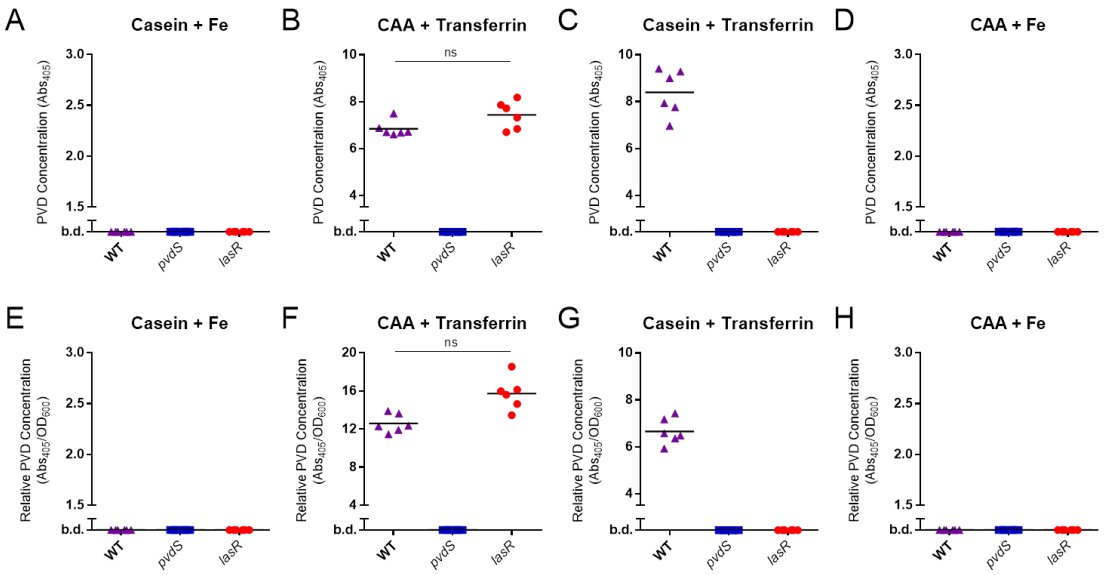

Figure S2 (Related to Figures 1 and 2). Total and relative pyoverdine (PVD) concentrations in WT, *pvdS*, and *lasR* monocultures after 48 hours of incubation in different media. Total PVD concentrations (Abs_{405}) in **(A)** iron-supplemented casein medium, **(B)** iron-depleted CAA medium, **(C)** iron-depleted casein medium, **(D)** iron-supplemented CAA medium. Relative PVD concentrations (PVD concentration per cell, Abs_{405}/OD_{600}), **(E)** in iron-supplemented casein medium, **(F)** in iron-depleted CAA medium, **(G)** in iron-depleted casein medium, **(H)** in iron-supplemented CAA medium. (For comparisons, Kruskal-Wallis test with Dunn's correction was used; ns=not significant, P>0.05; for all experiments N=6; b.d.: below detection). The total PVD concentrations are similar in both iron-depleted CAA **(B)**, and iron-depleted casein **(F)** media however, in iron-depleted CAA media WT and *lasR* produce more PVD per cell (Abs_{405}/OD_{600}). This higher energy spent per cell in the production of PVD might contribute to the lower biomass observed in iron-depleted CAA media compared to iron-depleted casein media (Figure 1).

Methods for pyoverdine concentration: PVD concentration measurements are done after 48 hours of growth in 37°C shaker by centrifuging the cells at 14000 r.p.m. for 4 minutes (Eppendorf Centrifuge 5418) and collecting the supernatant, measuring their absorbance at 405nm (Abs_{405}) in optical cuvettes as 1:10 dilutions with PBS solutions in a Thermo Spectronic Helios δ spectrophotometer.

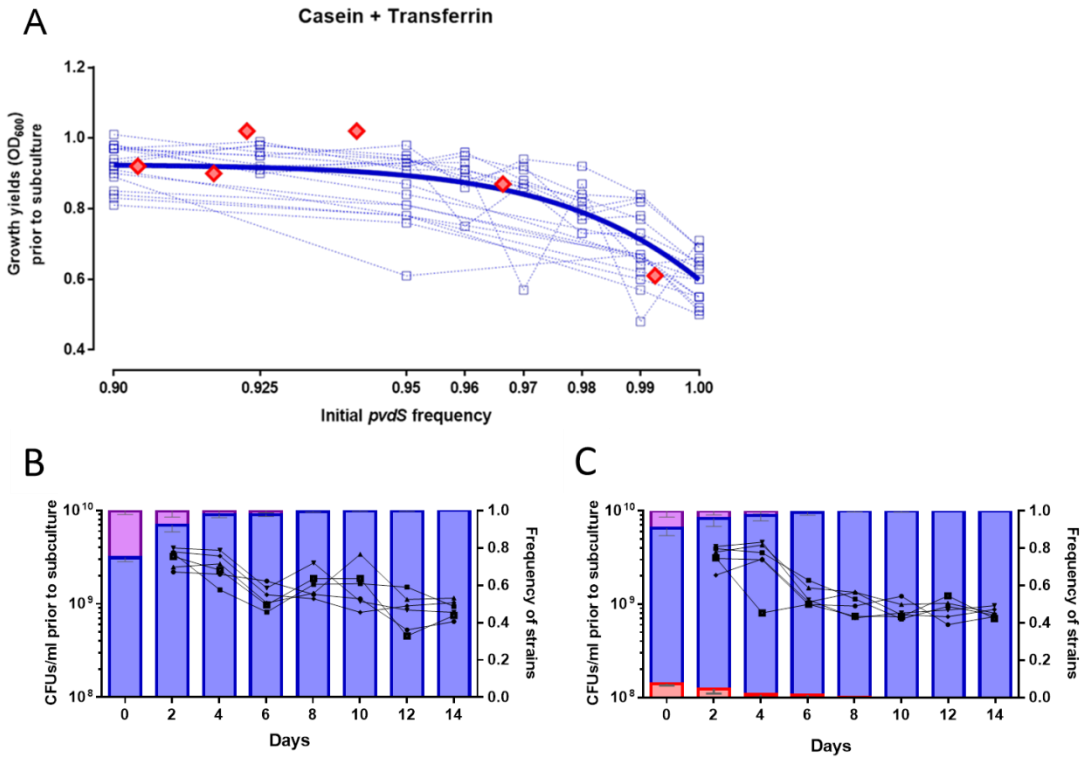

Figure S3 (Related to Figure 3). Decrease in population size caused by *pvdS* domination. (A) Effect of the initial frequency of *pvdS* in co-cultures with WT, on the overall growth yields of the population. Each blue square represents one short term competition (48 hours) in iron-depleted casein media (Casein + Transferrin). Initial frequencies of *pvdS* are shown in the 'X' axis (curve indicates the log regression of these short term competitions). Red diamonds show the OD_{600} measurements and matching inoculum frequencies of *pvdS* mutant from different co-cultures of the 18th day of the experiment shown in Figure 3D. Mann-Whitney two-tailed test of OD_{600} values of the cultures with 3% WT and 97% *pvdS* vs. 100% WT, P=0.1316; and OD_{600} of the cultures with 2% WT and 98% *pvdS* vs 100% WT, P<0.05. This comparison allows us to conclude that at frequencies above 97% of *pvdS* a significant decrease in population densities is observed. Propagations of WT+*pvdS* **(B)**, and WT+*pvdS*+*lasR* cultures **(C)** in iron-depleted casein media. 'X' axes show the days of propagation and 'Y' axes represent the frequency of each strain (the initial frequencies are shown at day 0). **(B)** Frequency changes of WT (purple bars) and *pvdS* (blue bars) in WT+*pvdS* co-cultures shown as stacked bars (N=6, Means ± SD) (right 'Y' axes) and the growth yields (CFUs/ml) of 6 biological replicates are shown as black lines (left 'Y' axes). **(C)** Frequency changes of WT (purple bars), *pvdS* (blue bars), and *lasR* (red bars) in WT+*pvdS*+*lasR* co-cultures shown as stacked bars (N=6, Means ± SD) (right 'Y' axes) and the growth yields (CFUs/ml) of 6 biological replicates are shown as black lines (left 'Y' axes).

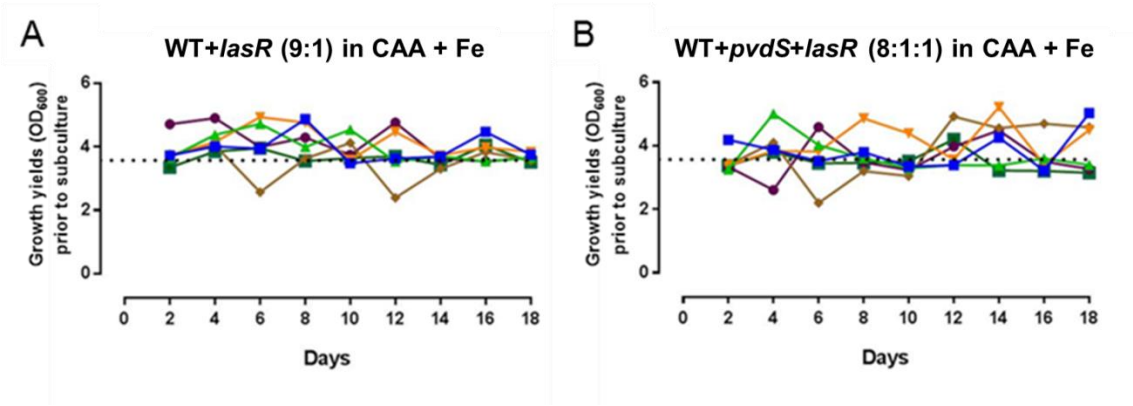

Figure S4 (Related to Figures 3 and 4). Propagations of WT+*lasR* and WT+*pvdS*+*lasR* co-cultures in medium where none of the traits are required, iron-supplemented CAA medium (CAA + Fe). **(A)** WT and *lasR* co-culture initially mixed (9:1) in iron-supplemented CAA medium. **(B)** WT, *pvdS*, and *lasR* co-culture initially mixed (8:1:1) in iron-supplemented CAA medium. 'X' axes show the days of propagations to fresh media. 'Y' Axes show the growth yields as OD_{600} at each time point, each colored line indicates one propagated culture (N=6), dash lines indicate the monoculture WT growth yields in the same medium (mean=3.57, ±SD=0.357, N=6).

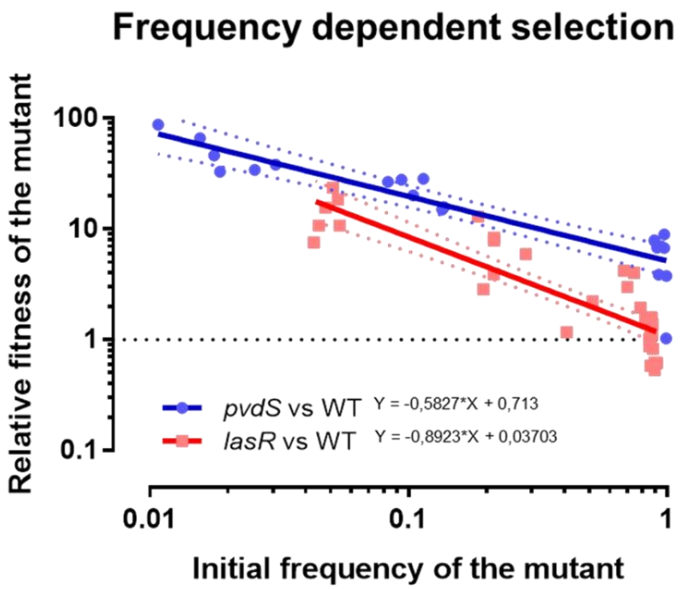

Figure S5 (Related to Figures 4 and 6). Frequency-dependent selection for *pvdS* and *lasR*. The change in relative fitness of either mutant in relation to their initial frequencies in co-culture with WT in iron-depleted or iron-supplemented casein media for *pvdS* (blue circles) or *lasR* (red squares), respectively. These results show that the cheating magnitudes of both mutants are frequency dependent, however, the effect of the initial frequency to their relative fitness values differ drastically. The cheating behavior of these two mutants is different, while *pvdS* cheats even at very high frequencies (~97%), *lasR* ceases to cheat at frequencies above ~85%. 'X' axis shows the frequencies of *pvdS* or *lasR* in the beginning of the competition with WT. 'Y' axis shows the relative fitness values of *pvdS* or *lasR* over WT after 48h of incubation. Lines indicate linear regressions; slopes of the lines are shown on the figure (Comparison of the lines: F=8,525, DFn=1, DFd=52, **=P=0,0052; the lines are significantly different). Red and blue dots indicate the 95% confidence intervals of the corresponding lines. The gray dotted line indicates no change in relative fitness (no cheating, relative fitness=1).

Mathematical Model 1 - Simple 3-way public goods model

We define the fitness of a cooperator and two cheaters mixed in an environment where the two traits that these mutants cheat on are necessary as:

$$\omega_{coop} = \omega_0 + b_1 (1 - p_{ch1}) + b_2 (1 - p_{ch2}) - c_1 - c_2 \quad (1)$$

$$\omega_{ch1} = \omega_0 + b_1 (1 - p_{ch1}) + b_2 (1 - p_{ch2}) - c_2 \quad (2)$$

$$\omega_{ch2} = \omega_0 + b_1 (1 - p_{ch1}) + b_2 (1 - p_{ch2}) - c_1 \quad (3)$$

The change in the mean fitness is given by:

$$\bar{\omega} = \Sigma_i \, p_i(t) \, \omega_i = \omega_0 + p_{coop}(t) \, \omega_{coop} + p_{ch1}(t) \, \omega_{ch1} + p_{ch2}(t) \, \omega_{ch2} \quad (4)$$

$$= \omega_0 + (b_1 - c_1) (1 - p_{ch1}(t)) + (b_2 - c_2) (1 - p_{ch2}(t)) \quad (5)$$

As can be seen from the fitness definitions (equations (1), (2), and (3)) of these three players, the cheaters always have a higher fitness than the cooperator due to the costs (c_1 or c_2) saved. Assuming a homogeneous environment, and ignoring stochastic effects, the population changes according to the replicator equation system:

$$dp_{coop} / dt = p_{coop}(t) (\omega_{coop} - \bar{\omega}) = p_{coop}(t) (- c_1 \, p_{ch1}(t) - c_2 \, p_{ch2}(t)) \quad (6)$$

$$dp_{ch1} / dt = p_{ch1}(t) (\omega_{ch1} - \bar{\omega}) = p_{ch1}(t) (c_1 (1 - p_{ch1}(t)) - c_2 \, p_{ch2}(t)) \quad (7)$$

$$dp_{ch2} / dt = p_{ch2}(t) (\omega_{ch2} - \bar{\omega}) = p_{ch2}(t) (c_2 (1 - p_{ch2}(t)) - c_1 \, p_{ch1}(t)) \quad (8)$$

As shown in Figure 5A, the predicted mean fitness ($\bar{\omega}$) and final frequencies of the different strains in the population assuming different c_1/c_2 ratios. It can be easily seen that cooperators will always go extinct, and that the two cheaters can only co-exist when $c_1 = c_2$.

Whenever $c_1 \neq c_2$, then the cheater that produces the more costly trait will lose. Therefore, the relation between c_1 and c_2 determines which cheater will dominate the population, independently of the benefits (b_1 and b_2) of these cooperative traits. On the other hand, the mean fitness, $\bar{\omega}$, is affected by the difference between b and c values of each trait.

We note that this theoretical analysis assumes infinite population, and the effects of fluctuating population size and of bottlenecks [25], which occur in the experimental populations at each passage, are beyond the scope of this simple model. Nevertheless, when full dominance of a cheater is predicted to occur, one would expect that, in a finite population, its yield will be lower than that of the WT monoculture and will be set by the values of the benefits b_1 or b_2.

For the simulation of the four scenarios corresponding to the conditions in Figure 3 (Figure S6A-D), in panels (A) and (C), the cooperator for both traits (WT) and the cheater of the 1st cooperative trait compete ($p_{coop}(0) = 0.9$ and $p_{ch1}(0) = 0.1$), while the cheater of the 2nd cooperative trait is absent ($p_{ch2}(0)=0$), whereas in panels (B) and (D) all three strains compete ($p_{coop}(0) = 0.8$ and $p_{ch1}(0) = p_{ch2}(0) = 0.1$). In panels (A) and (B), only the 1st cooperative trait is necessary ($b_1 > c_1 > 0$, whereas $b_2 = c_2 = 0$), while in panels (C) and (D) both traits are required ($c_2 > c_1 > 0$ and $b_1 > b_2 > 0$). The mean fitness, $\bar{\omega}$,of the entire population (shown as black lines in Figure 7 and Figure S6) as is a function of b and c values which are the biomass gain due to benefiting from the cooperative action (b), and the energy spent to the cooperative action (c). The time scale of the simulations is arbitrary, but since the cumulative number of cell divisions depends on the environment, the simulated time was higher in the iron-supplemented casein media (Casein + Fe) than iron-depleted casein media (Casein + Transferrin) [26,27]. The cumulative number of cell divisions was estimated from the final number of cells in the competitions in Figure 2. For the same time period (48 hours after inoculation) the cumulative number of cell divisions was significantly higher in medium where only elastase was required (Casein + Fe) than in conditions when both traits are necessary (Casein + Transferrin) (Figure 1 and Figure 3). ω_0, b_1, and b_2 are chosen to reflect the growth yields in Figure 1.

<u>Mathematical Model 2</u> - Simple 3-way public goods model including quorum sensing

We modelled the effect of quorum sensing (QS) on fitness equations by assuming a Hill function where the cost (c_1) and benefit (b_1) of the 1st cooperative trait are sharply reduced when the frequency the cheater for the 1st cooperative trait (p_{ch1}) reaches a given threshold value (th), as:

$$\omega_{coop} = \omega_0 + b_1 (1 - p_{ch1}) (1 / (1 + (p_{ch1} / th)^n)) + b_2 (1 - p_{ch2}) - c_1 (1 / (1 + (p_{ch1} / th)^n)) - c_2 \quad (9)$$

$$\omega_{ch1} = \omega_0 + b_1 (1 - p_{ch1}) (1 / (1 + (p_{ch1} / th)^n)) + b_2 (1 - p_{ch2}) - c_2 \quad (10)$$

$$\omega_{ch2} = \omega_0 + b_1 (1 - p_{ch1}) (1 / (1 + (p_{ch1} / th)^n)) + b_2 (1 - p_{ch2}) - c_1 (1 / (1 + (p_{ch1} / th)^n)) \quad (11)$$

The dynamics of mean fitness, which we also plot in the Figure 7, is given by:

$$\bar{\omega} = \omega_{0+} ((b_1 - c_1) (1 - p_{ch1}(t)) / (1 / (1 + (p_{ch1} / th)^n))) + (b_2 - c_2) (1 - p_{ch2}(t)) \quad (12)$$

In this case, fixation of one mutant can only happen if $c_1 < c_2$. When $c_1 \geq c_2$, both cheaters can co-exist in the population (Figure 5B).

As shown in Figure 7, the simulations of the modified model including QS for the four experimental conditions used here predict accurately the frequency dynamics. Figure S6E-I represent the predictions, according to our model, of other possible scenarios with different relationships between the costs, which can be tested experimentally in the future.

Table S1 (Related to Figures 5 and 7) - Model Parameters

Symbols	Descriptions
c_1	Cost of the 1st cooperative trait
c_2	Cost of the 2nd cooperative trait
b_1	Benefit gained from the 1st cooperative trait
b_2	Benefit gained from the 2nd cooperative trait
ω_0	Fitness without the additional fitness effects of the cooperative traits (basal fitness)
ω_{coop}	Fitness of the cooperator of the both cooperative traits
ω_{ch1}	Fitness of the cheater of the 1st cooperative trait
ω_{ch2}	Fitness of the cheater of the 2nd cooperative trait
$\bar{\omega}$	Mean fitness of the entire population (A proxy for OD_{600} or CFUs/ml)
p_{coop}	Frequency of the cooperator of the both cooperative traits in the entire population
p_{ch1}	Frequency of the cheater of the 1st cooperative trait in the entire population
p_{ch2}	Frequency of the cheater of the 2nd cooperative trait in the entire population
	Parameters considered only in the model with QS (Mathematical Model 2)
th	Quorum threshold (as a function of the non-QS strain frequency)
n	Hill coefficient for the slope of the inhibition of the QS-regulated public good

When only the cooperator of both cooperative traits (e.g. WT) and the cheater of the 2nd cooperative trait (which is not regulated by QS, e.g. *pvdS*) are in competition, the cheater wins and reaches fixation as in the triple co-culture scenario. The results are the same whether the 1st cooperative trait is regulated by QS, or not (Figure S6E); and the final mean fitness becomes:

$$\bar{\omega} = \omega_0 + b_1 - c_1 \quad (13)$$

When only two cheaters are in competition (1:1), the cheater that saves the greater cost (here, the cheater of the 2nd cooperative trait since $c_2 > c_1$) wins the competition and reaches fixation regardless of QS regulation of the 1st cooperative trait (Figure S6F), and the final mean fitness becomes:

$$\bar{\omega} = \omega_0 + b_1 - c_1 \quad (14)$$

When the cooperator of the both cooperative traits (e.g. WT) is competing with two mutants under conditions where the costs of both traits are equal ($c_1 = c_2$), both cheaters increase in frequency until both of them reach 50% of the population (Figure S6G), similarly with or without QS regulation of the 1st cooperative trait, and the final mean fitness becomes:

$$\bar{\omega} = \omega_0 + ½ (b_1 + b_2 - c_1 - c_2) \quad (15)$$

When the cooperator of the both cooperative traits (e.g. WT) is competing with two mutants under conditions where the $c_1 > c_2$, then the more drastic tragedy-inducing cheater becomes the winner of the 3-way competition. In this case, when the 1st cooperative is not regulated by QS, the cheater of the 1st cooperative trait wins the 3-way competition causing a drastic collapse (Figure S6H); and the final mean fitness becomes:

$$\bar{\omega} = \omega_0 + b_2 - c_2 \quad (16)$$

However, when the 1st cooperative trait is regulated by QS, the cheater of the 1st cooperative trait, while it still wins the competition, it only increases in frequency until the QS threshold (th=0.8) and thus, cannot reach fixation (Figure S6I); and the mean final fitness becomes:

$$\bar{\omega} = \omega_0 + (b_1 - c_1)\,(0.4) + (b_2 - c_2)\,(0.8) \quad (17)$$

As a result, the cooperator of the both cooperative traits (e.g. WT) persists in the population. Therefore, presumably, the population has a greater chance to recover if the

environmental conditions change. In conclusion, the QS regulation becomes relevant only under conditions where the mutant for the QS-regulated trait (here the cheater of the 1st cooperative trait) is not completely outcompeted.

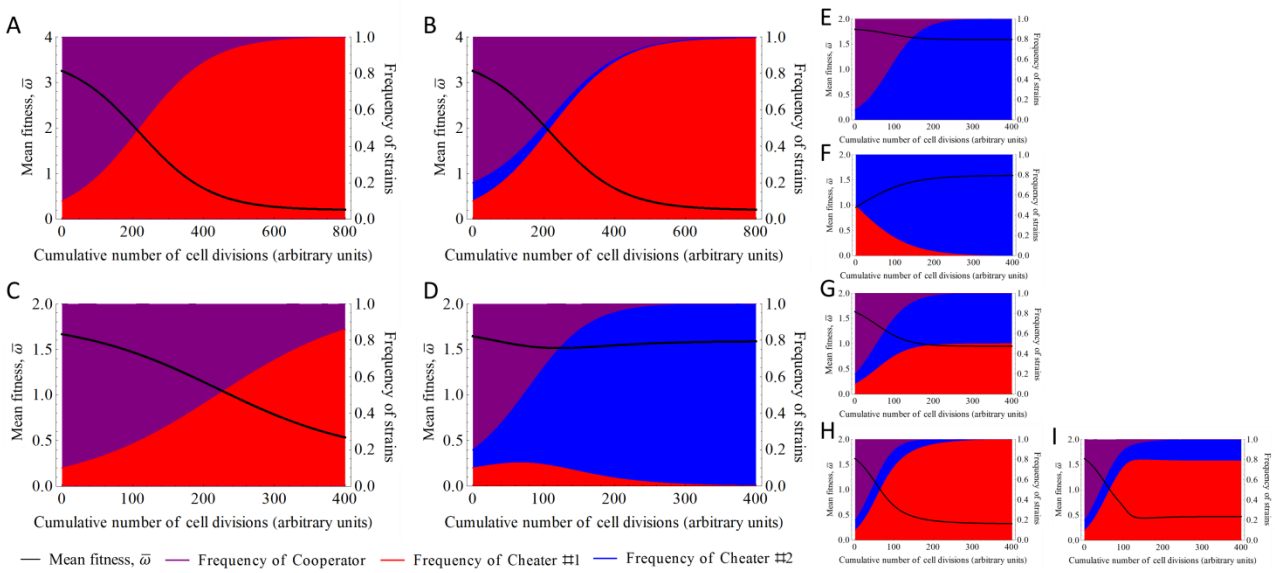

Figure S6 (Related to Figures 5 and 7). Simulations of alternative scenarios by using Mathematical Model 1 and 2. (A), **(B)**, **(C)**, and **(D)** are the simulations of the four scenarios of Figure 3, as in Figure 7 but without quorum sensing regulation of the 1st cooperative trait. **(E)** Simulation with two strains, full cooperator (WT) + cheater for the 2nd cooperative trait, under conditions where both public goods are produced and $c_2>c_1$. **(F)** Simulation with the two cheaters competing with each other, under conditions where both public goods are produced and $c_2>c_1$. **(G)** Simulation for a 3-way competition with the cooperator of the both cooperative traits competing with two cheaters, under conditions where both public goods are produced and $c_2=c_1$. **(H)** and **(I)** are the simulation for a 3-way competition with the cooperator of the both cooperative traits competing with two cheaters, without and with quorum sensing regulation of the 1st cooperative trait, respectively, under conditions where both public goods are produced and $c_1>c_2$. Axes are the same as in Figure 7. The values that are given to the parameters of the simulations are: **(A)** $p_{coop}(0)$=0.9, $p_{ch1}(0)$=0.1, pch2(0)=0, c_1=0.01, b_1=3.4, c_2=0, b_2=0, ω_0=0.2; **(B)** $p_{coop}(0)$=0.8, $p_{ch1}(0)$=0.1, $p_{ch2}(0)$=0.1, c_1=0.01, b_1=3.4, c_2=0, b_2=0, ω_0=0.2; **(C)** $p_{coop}(0)$=0.9, $p_{ch1}(0)$=0.1, $p_{ch2}(0)$=0, c_1=0.01, b_1=1.5, c_2=0.025, b_2=0.25, ω_0=0.1; **(D)** $p_{coop}(0)$=0.8, $p_{ch1}(0)$=0.1, $p_{ch2}(0)$=0.1, c_1=0.01, b_1=1.5, c_2=0.025, b_2=0.25, ω_0=0.1; **(E)** $p_{coop}(0)$=0.9, $p_{ch1}(0)$=0, $p_{ch2}(0)$=0.1, c_1=0.01, b_1=1.5, c_2=0.025, b_2=0.25, ω_0=0.1. The results are the same regardless if the 1st is considered to be regulated by QS (n=30, th=0.8) or not (n=0, th=0); **(F)** $p_{coop}(0)$=0, $p_{ch1}(0)$=0.5, $p_{ch2}(0)$=0.5, c_1=0.01, b_1=1.5, c_2=0.025, b_2=0.25, ω_0=0.1. The results are the same regardless if the 1st is considered to be regulated by QS (n=30, th=0.8) or not (n=0, th=0); **(G)** $p_{coop}(0)$=0.8, $p_{ch1}(0)$=0.1, $p_{ch2}(0)$=0.1, c_1=0.025, b_1=1.5, c_2=0.025, b_2=0.25, ω_0=0.1. The results were the same regardless if QS regulation for the 1st cooperative trait is considered (n=30, th=0.8) or not (n=0, th=0); **(H)** $p_{coop}(0)$=0.8, $p_{ch1}(0)$=0.1, $p_{ch2}(0)$=0.1, c_1=0.04, b_1=1.5, c_2=0.025, b_2=0.25, ω_0=0.1, n = 0, th = 0; **(I)** same as in (H) except n=30 and th=0.8, as QS regulation is considered for the 1st cooperative trait. Note that the values of parameters used in these simulations are chosen to reflect approximately the relation between the values observed in Figure 1, Figure 2.

Supplementary Methods

Bacterial strains. The strains used in this study were *Pseudomonas aeruginosa* WT strain PA01, PA01 *lasR* mutant harboring a gentamycin resistant gene inserted in *lasR* (*lasR::GmR*) [28], and PA01 *pvdS* mutant harboring a gentamycin resistance gene replacing the *pvdS* coding sequence (Δ*pvdS::GmR*) [29]. As the WT and *lasR* strains (which are isogenic) come from a different source than the *pvdS* strain and in the light of the recent work by Harrison and colleagues describing the remarkable heterogeneity among lab strains typically used in *P. aeruginosa* sociomicrobiology studies [30], we constructed a new *pvdS* deletion mutant using the WT strain used in this study as background (isogenic also with the *lasR* mutant) (see detailed description for the construction of the Δ*pvdS::StrR* below). This allowed us to determine whether there is a difference between the *pvdS* and the other two strains (WT and *lasR* strains) and to assess if there are any possible effects on the phenotypes described in this study. As shown in Figure S7, the growth yields of the newly constructed mutant, Δ*pvdS::StrR*, were not significantly different from the *pvdS* mutant used throughout our work (referred in Figure S7 as Δ*pvdS::GmR*) for any of the media used (Figure S7A-D). We have also determined the cheating capacity of the Δ*pvdS::StrR* against the WT, in the same conditions used in Figure 2 (Figure S7E-H). The cheating capacity of the Δ*pvdS::StrR* was not significantly different from the *pvdS* mutant used throughout our work (Figure S7). In agreement with the results presented throughout the present study both *pvdS* mutants increase in frequency in the media where pyoverdine is required but have no advantage against the WT in the media supplemented with iron. Moreover, Δ*pvdS::StrR* had no pyoverdine production in all four media as Δ*pvdS::GmR*.

Construction of a Δ*pvdS::StrR* mutant. We constructed a *pvdS* mutant by allelic replacement [31] of the *pvdS* coding sequence by a cassette containing the genes *strA* and *strB*, conferring resistance to streptomycin in the WT strain used in this study. Briefly, the *strAB* cassette from pKNG101, and approximately 700bp of the sequences upstream and downstream from the *pvdS* coding sequence (from WT PAO1) were amplified using primers ORB338, ORB339, ORB340, ORB341, ORB342, and ORB360. These PCR products were restricted, ligated and cloned in the vector pUC18 as a unique fragment *pvdS(5')-strAB-pvdS(3')*. This fragment was then cloned in the suicide vector pKNG101 [31], replacing the *strAB* cassette originally present in the vector, using the primers ORB344 and ORB345, and generating the plasmid pOZ1. Then pOZ1 was introduced into the WT PAO1 strain by tri-

parental conjugation [32–34], using *E. coli* λ pir (lab stock) and the helper plasmid pRK2013 [34,35], causing the insertion of the entire pOZ1 at the *pvdS* locus by a single site-specific recombination. Then, cells where a second site-specific recombination event causing the excision of pOZ1 occurred, were selected by plating on medium containing sucrose (to counterselect the *sacB* gene carried by pOZ1) and streptomycin (to select recombinants harbouring the version of *pvdS* replaced by *strAB*). The resulting strains were checked to carry the right Δ*pvdS::strAB* construction by PCR with primers ORB367 and ORB368.

List of primers

ORB338 ATAGGATCCGCAGGCAGAACAATTGCAG
ORB339 ATAGGATCCTTGCAGCAGATGCCCTAC
ORB340 TATACTAGTAGGCATAGGCTTGGTTATGC
ORB341 TATACTAGTCTGATCTTCAGATCCTCTACGC
ORB342 AAAACTAGTCAACGTCACCCATCTCAG
ORB360 TTTACTAGTGACAGTTGTTCCGACATG
ORB367 CAGAGCGCTTTCCCATGATCG
ORB368 CGCCGATTACGTCAGGCATC

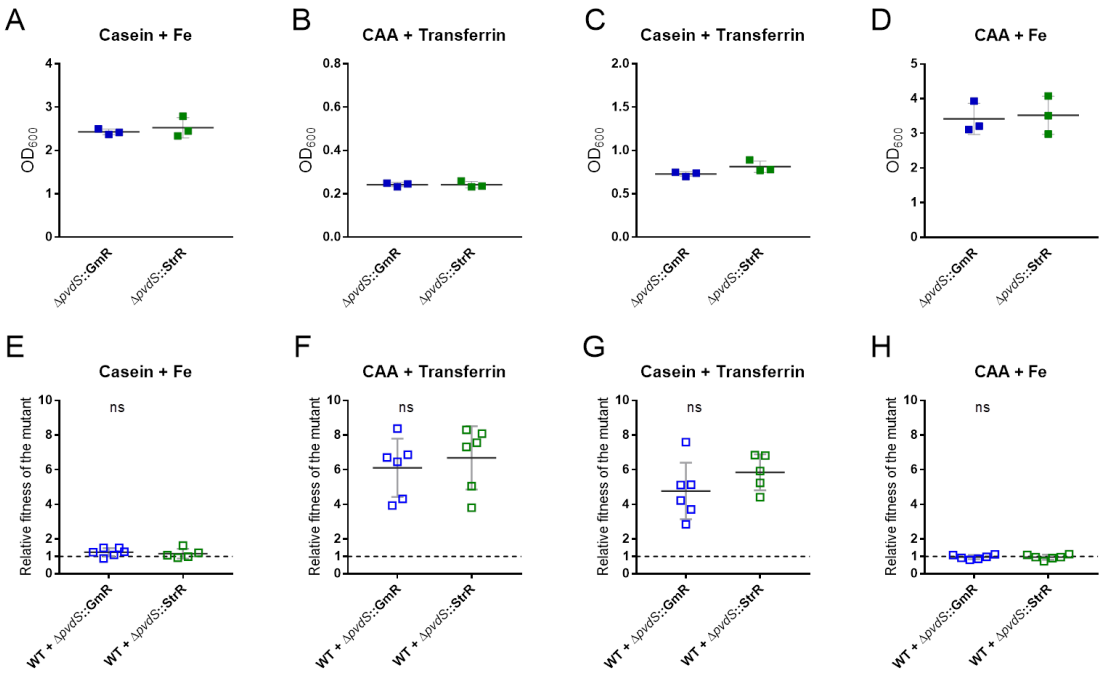

Figure S7 (Related to Materials and Methods – Bacterial strains). The growth yields and cheating capacities of the newly constructed Δ*pvdS*::*StrR* mutant are not different from the Δ*pvdS*::*GmR* used in this study. (A), **(B)**, **(C)**, and **(D)** are the growth yields (OD_{600}) comparisons of the monocultures of *pvdS* mutant (Δ*pvdS*::*GmR*) (blue squares) used in this study and the newly constructed *pvdS* mutant (Δ*pvdS*::*StrR*) (green squares) in iron-supplemented casein (A), iron-depleted CAA (B), iron-depleted casein (C), and iron-supplemented CAA media (D). **(E)**, **(F)**, **(G)**, and **(H)**, are the relative fitness values of each mutant from the competitions between WT and Δ*pvdS*::*GmR* (blue squares) (with the initial frequencies of 9:1), and between WT and Δ*pvdS*::*StrR* (green squares) (with the initial frequencies of 9:1) in the same media as in (A), (B), (C), and (D), respectively.

Supplemental References:

1. Wang, M., Schaefer, A.L., Dandekar, A.A., and Greenberg, E.P. (2015). Quorum sensing and policing of *Pseudomonas aeruginosa* social cheaters. Proc. Natl. Acad. Sci. 112, 2187–2191.
2. Dandekar, A.A., Chugani, S., and Greenberg, E.P. (2012). Bacterial quorum sensing and metabolic incentives to cooperate. Science 338, 264–266.
3. Asfahl, K.L., Walsh, J., Gilbert, K., and Schuster, M. (2015). Non-social adaptation defers a tragedy of the commons in *Pseudomonas aeruginosa* quorum sensing. ISME J. 9, 1734–1746.
4. Griffin, A.S., West, S. A., and Buckling, A. (2004). Cooperation and competition in pathogenic bacteria. Nature 430, 1024–1027.
5. Ross-Gillespie, A., Gardner, A., West, S. A., and Griffin, A.S. (2007). Frequency dependence and cooperation: theory and a test with bacteria. Am. Nat. 170, 331–42.
6. Harrison, F., Paul, J., Massey, R.C., and Buckling, A. (2008). Interspecific competition and siderophore-mediated cooperation in *Pseudomonas aeruginosa*. ISME J. 2, 49–55.
7. Brockhurst, M. A., Buckling, A., Racey, D., and Gardner, A. (2008). Resource supply and the evolution of public-goods cooperation in bacteria. BMC Biol. *6*, 20.
8. Kümmerli, R., Gardner, A., West, S.A., and Griffin, A.S. (2009). Limited dispersal, budding dispersal, and cooperation: an experimental study. Evolution 63*,* 939–949.
9. Kümmerli, R., Jiricny, N., Clarke, L.S., West, S.A., and Griffin, A.S. (2009). Phenotypic plasticity of a cooperative behaviour in bacteria. J. Evol. Biol. 22, 589–98.
10. Kümmerli, R., Griffin, A.S., West, S. A., Buckling, A., and Harrison, F. (2009). Viscous medium promotes cooperation in the pathogenic bacterium *Pseudomonas aeruginosa*. Proc. Biol. Sci. 276, 3531–3538.
11. Ross-Gillespie, A., Gardner, A., Buckling, A., West, S. A., and Griffin, A.S. (2009). Density dependence and cooperation: theory and a test with bacteria. Evolution 63, 2315–25.
12. Kümmerli, R., van den Berg, P., Griffin, A. S., West, S. A., and Gardner, A. (2010). Repression of competition favours cooperation: experimental evidence from bacteria. J. Evol. Biol. 23, 699–706.
13. Kümmerli, R., and Brown, S.P. (2010). Molecular and regulatory properties of a public good shape the evolution of cooperation. Proc. Natl. Acad. Sci. U. S. A. 107, 18921–

18926.

14. Jiricny, N., Diggle, S.P., West, S.A., Evans, B.A., Ballantyne, G., Ross-Gillespie, A., and Griffin, A.S. (2010). Fitness correlates with the extent of cheating in a bacterium. J. Evol. Biol. 23, 738–747.
15. Harrison, F., and Buckling, A. (2011). Wider access to genotypic space facilitates loss of cooperation in a bacterial mutator. PLoS One 6, e17254.
16. Dumas, Z., and Kümmerli, R. (2012). Cost of cooperation rules selection for cheats in bacterial metapopulations. J. Evol. Biol. 25, 473–484.
17. Dumas, Z., Ross-Gillespie, A., and Kümmerli, R. (2013). Switching between apparently redundant iron-uptake mechanisms benefits bacteria in changeable environments. Proc Biol Sci 280, 20131055.
18. Ross-Gillespie, A., Dumas, Z., and Kümmerli, R. (2015). Evolutionary dynamics of interlinked public goods traits: An experimental study of siderophore production in *Pseudomonas aeruginosa*. J. Evol. Biol. 28, 29–39.
19. Kümmerli, R., Santorelli, L.A., Granato, E.T., Dumas, Z., Dobay, A., Griffin, A.S., and West, S.A. (2015). Co-evolutionary dynamics between public good producers and cheats in the bacterium *Pseudomonas aeruginosa*. J. Evol. Biol. 28, 2264–74.
20. Ghoul, M., West, S.A., McCorkell, F.A., Lee, Z.-B.B., Bruce, J.B., and Griffin, A.S. (2016). Pyoverdin cheats fail to invade bacterial populations in stationary phase. J. Evol. Biol. 29, 1728–1736.
21. Leinweber, A., Fredrik Inglis, R., and Kümmerli, R. (2017). Cheating fosters species co-existence in well-mixed bacterial communities. ISME J. 11, 1179–1188.
22. Kümmerli, R., and Ross-Gillespie, A. (2013). Explaining the sociobiology of pyoverdin producing *Pseudomonas*: A comment on Zhang and Rainey (2013). Evolution 11, 3337–3343.
23. Demott, B.J., and Dincer, B. (1976). Binding added iron to various milk proteins. J. Dairy Sci. 59, 1557–1559.
24. Smialowska, A., Matia-Merino, L., and Carr, A.J. (2017). Oxidative stability of iron fortified goat and cow milk and their peptide isolates. Food Chem. 237, 1021–1024.
25. McAvoy, A., Fraiman, N., Hauert, C., Wakeley, J., and Nowak, M.A. (2017). Public goods games in populations with fluctuating size. arXiv:1709.03630
26. Lee, D.H., Feist, A.M., Barrett, C.L., and Palsson, B. (2011). Cumulative number of cell divisions as a meaningful timescale for adaptive laboratory evolution of *Escherichia coli*.

PLoS One 6, 1–8.

27. Luria, S., and Delbrück, M. (1943). Mutations of bacteria from virus sensitivity to virus resistance. Genetics 28, 491–511.
28. Popat, R., Crusz, S.A., Messina, M., Williams, P., West, S.A., and Diggle, S.P. (2012). Quorum-sensing and cheating in bacterial biofilms. Proc. Biol. Sci. 279, 4765–4771.
29. Ochsner, U.A., Johnson, Z., Lamont, I.L., Cunliffe, H.E., and Vasil, M.L. (1996). Exotoxin A production in *Pseudomonas aeruginosa* requires the iron-regulated *pvdS* gene encoding an alternative sigma factor. Mol. Microbiol. 21, 1019–1028.
30. Harrison, F., McNally, A., da Silva, A.C., Heeb, S., and Diggle, S.P. (2017). Optimised chronic infection models demonstrate that siderophore “cheating” in *Pseudomonas aeruginosa* is context specific. ISME J. 11, 2492–2509.
31. Kaniga, K., Delor, I., and Cornelis, G.R. (1991). A wide-host-range suicide vector for improving reverse genetics in Gram-negative bacteria: inactivation of the *blaA* gene of *Yersinia enterocolitica*.
32. Filloux, A., and Ramos, J.-L. eds. (2014). *Pseudomonas* Methods and Protocols (New York, NY: Springer New York).
33. Muhl, D., and Filloux, A. (2014). Site-Directed Mutagenesis and Gene Deletion Using Reverse Genetics. In, pp. 521–539.
34. Sana, T.G., Laubier, A., and Bleves, S. (2014). Gene Transfer: Conjugation. In, pp. 17–22.
35. Figurski, D.H., and Helinski, D.R. (1979). Replication of an origin-containing derivative of plasmid RK2 dependent on a plasmid function provided in trans. Proc. Natl. Acad. Sci. U. S. A. 76, 1648–52.